# A Novel Deep-Learning Based Segmentation Of Kidney Tumor

Ashlin Deepa R. N
Computer Science and Engineering
Gokaraju Rangaraju Institute of Engineering and Technology
Hyderabad, India
rndeepa.pradeep@gmail.com

T . Sai chand
Computer Science and Engineering
Gokaraju Rangaraju Institute of Engineering and Technology
Hyderabad, India
saichand8402@gmail.com

S . Sanjay
Computer Science and Engineering
Gokaraju Rangaraju Institute of Engineering and Technology
Hyderabad, India
sanjaysundaragiri@gmail.com

S . Vamshi
Computer Science and Engineering
Gokaraju Rangaraju Institute of Engineering and Technology
Hyderabad, India
vamshisamineni3@gmail.com

V . M . Mahith
Computer Science and Engineering
Gokaraju Rangaraju Institute of Engineering and Technology
Hyderabad, India
mahith47@gmail.com

***Abstract*—➢ A crucial step in cutting-edge surgical planning and radiomic analysis is precise kidney and renal tumor segmentation. Using diagnostic images like those from computed tomography (CT) scans, the kidney and tumor can be precisely segmented for effective treatment. As a result, segmentation is essential for establishing a connection between the tumor and its surgical outcome and assisting physicians in developing treatment plans that are more precise. Because of advancements in biomedical image segmentation algorithms, we were able to create an accurate automated segmented mask. For the purpose of segmenting the tumor and creating tumor output masks in this instance, we are making use of SqueezeNets, ResNet, and 3D U-Net. In real time,the deep learning models take a lot of time to compute to resolve this issue we're using SqueezeNet which takes less compute time and reduces the cost of computation.**

**Keywords—Image segmentation, Kidney tumor, Medical image segmentation, SqueezeNet, Deep Learning**

## I. Introduction

Kidney cancer is a disease that starts in the kidneys. Also known as renal tumors, kidney tumors can be benign or cancerous. It occurs when healthy kidney cells grow out of control and form a lump, or tumor, in one or both kidneys [1]. The majority are unnoticeable while you are receiving treatment for another condition because they do not cause symptoms. The kidneys, which are organs in the abdomen, aid the body in maintaining a healthy balance of chemicals like sodium, potassium, and calcium by removing waste and excess water from the blood and passing it out as urine. By encouraging the bone marrow to produce red blood cells, hormones produced by the kidneys also help control blood pressure.

Kidney cancer is thought to occur when a tumor in the kidney is malignant. Anemia, a lack of appetite, blood in the urine, lower back pain, and an unexpected weight loss are all signs of kidney cancer. Renal cancer can also be caused by obesity. One side of the kidney's abdomen may bulge if it has developed abnormally. The risk of spreading to the entire kidney is very gradual due to their slow growth. Renal cell carcinoma (RCC) is the most common type of kidney cancer in adults. The lining of renal tubules, which are small tubes in the kidney, is typically where RCC begins. RCC can spread to the brain, lungs, bones, or other parts of the body, but it usually stays in the kidney.

The stages of kidney cancer range from I (the initial stage) to IV (the final stage). In general, there is less cancer if the number is lower. spread. A higher number, such as stage IV, indicates greater cancer spread. Within a stage, an earlier letter (or number) denotes a lower level. Despite the fact that every person's experience with cancer is unique, cancers in the same stage typically share a similar outlook and are frequently treated in a similar manner [2].

Medical image segmentation aims to provide pixel-level semantic interpretation by automatically generating segmentation masks for organs and tumors. Nevertheless, there are organic characteristics such as varying appearances, varying sizes, locational unpredictability, and numerous variations. Contrast agent-based medical image segmentation is more advanced than traditional semantic photo segmentation. Deep learning introduced area to address these issues [3]. The Kidney Tumor Segmentation Challenge (KiTS) and the Liver Tumor Segmentation Challenge (LiTS) are two image segmentation challenges in which convolutional neural networks have been utilized. The implementation of 3D convolution kernels, the elimination of feature extractors, and the addition of dense connections are just a few of the numerous efforts that have been made to enhance methods for medical image segmentation since the introduction of UNet [3].

Recent research on deep neural networks has primarily focused on improving accuracy. Most of the time, there are multiple DNN (deep neural network) architectures that can get a certain level of accuracy. There are at least three advantages to smaller DNN architectures with the same level of precision: 1) Smaller DNNs require less server communication during distributed training. 2) Smaller DNNs require less bandwidth to transfer a brand-new model from the cloud to an autonomous vehicle. 3) Utilizing smaller DNNs on hardware with limited memory, such as FPGAs, is simpler. To provide all of these advantages, we suggest the compact DNN architecture SqueezeNet. On ImageNet,

SqueezeNet achieves AlexNet-level accuracy with 50 times fewer parameters. Model compression techniques can also be used to compress SqueezeNet to less than 0.5 MB, which is 510 times smaller than AlexNet[6].
In this paper, we used squeezeNet, which computes faster than the other architectures that can be used to make segmented masks.

## II. LITERATURE SURVEY

Zhou, Tajbakhsh, Siddique, and Liang worked on medical image segmentation with the U-net++ algorithm. It is used for semantic segmentation, for example. This overcomes two limitations with an effective ensemble of U-Nets of varying depths that partially share an encoder and co-learn simultaneously using deep learning: 1) the unknown depth of the network; Secondly, their skip connections impose a fusion scheme restriction that is unnecessary. Feature fusion becomes extremely adaptable by redesigning skip connections to aggregate features. This model outperformed across a variety of datasets for semantic segmentation, earning a dice score of 0.9236.
The dilated dense method for segmenting a MR image of the right ventricle was developed by Heming, Zheng, and Xingrong. It is widely used to process useful features. The outcome is more stable and precise than that of other algorithms. The issue of overfitting has also been resolved, and the train set's dice metric is now 0.91, while the test set's is 0.90.
The AlexNet algorithm for diagnosing diabetic retinopathy was developed in collaboration between Abbas cheddad and Qian wu. Using some image segmentation techniques, the fundus image can be divided up into the optic disc, the blood vessels, and other parts. Ten rounds were run for each model using GoogleNet, VGG19, and Resnet50. On the dice, An got a 0.92.

G. Aruna and Bikrant Sarmah worked together to create a low-cost IoT-based cold storage management system to overcome the difficulties of using machine learning algorithms like U-Net to track food quality and quantity. It is utilized for the calculation and detection of atmospheric methane, which is a sign of food freshness and quality. resulting in a dice score of 0.94.

The majority of the work that was carried out by llkay Oksuz, James R. Clough, Bram ruijsink, Esther puyol anton, Aurelian bustin, Gastao cruz, Claudia Prieto, Andrew P. King, and Julia A. Schnabel was related to biomedical imaging sciences. We developed an end-to-end segmentation network and used U-Net algorithms to work on cardiac MR segmentation together. It consisted of three distinct tasks and utilized 500 2D+ time MR acquisitions from the UK biobank dataset: final image segmentation, correction of artifacts, and artifact detection. We finally achieved high segmentation accuracy and satisfactory image quality with a dice score of 0.93.

Image segmentation on magnetic resonance (MR) images was worked on by Chengjia wang, Agisilaos chartsias, Scott Semple, David E. Newby, Rohan Dharmakumar, and Giorgos Papanastasiou employing the DAFNet (Dense Attention Fluid Network) algorithm. And presented a strategy for segmenting the modality of interest with greater accuracy than a single input model. The imaging factor also records intensity characteristics across various data modalities and is utilized for image reconstruction. Input slicing and temporal pairing are learned dynamically. obtained a final score of 0.85 on the dice.

## III. METHODOLOGY

We go into detail about the proposed method in this section. It includes the dataset's source, the model architecture, and the methods used to pre-process the data.

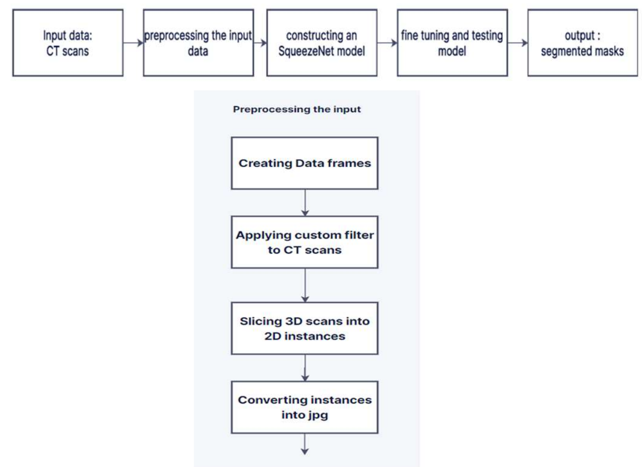

Fig. 1. Model Architecture

All of the computed tomography scans were provided by the kidney tumor segmentation 2019 grand challenge, which was held at the Medical Image Computing and Computer Assisted Intervention conference (Miccai)[7]. The.nii.gz file extension is used to save the CT scans. The is typically where multidimensional neuroimaging data are kept. format NII (or NIfTI). The majority of packages also support reading zip-compressed NIfTI files, which should have the extension.NII.gz [8]. The 2D visualization of the 3D CT scan

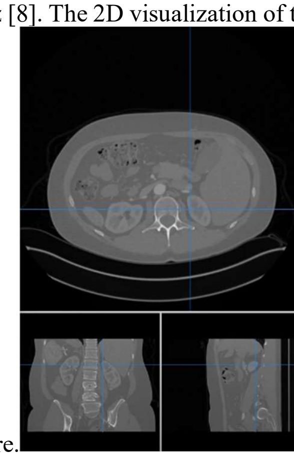

can be found here.
Fig 2: CT scan in .nii format

These files were processed with the help of the nibabel library. Data frames were made after libraries were imported, and a standard custom filter was used to make the component in the scan better. After that, the three-dimensional scans were broken up into two instances and saved as jpg files.

Deep learning produces very significant outcomes when dealing with large datasets. Our model was built with squeezeNet and u-net learner. SqueezeNet is a convolutional neural network with 18 layers. The ImageNet database can be used to load a pretrained version of the network that has been trained on more than one million images. Images can be classified into one thousand object categories using the pretrained network, including keyboard, mouse, pencil, and numerous animals.

The Fire module is the building block of SqueezeNet. It has two layers: a squeeze layer and an expand layer. A SqueezeNet is made up of stacked fire modules and pooling layers. The feature map size is the same for both the squeeze layer and the expand layer, with the squeeze layer decreasing the depth and the expand layer increasing it. The bottleneck layer (squeezing) and expansion behaviors are common in neural architectures. Another common pattern is to reduce the size of the feature map while increasing its depth[9] in order to achieve high-level abstract. The following are included in a Fire module: an expand layer that feeds into a squeeze convolution layer and has a mix of 1x1 and 3x3 convolution filters. We gradually increase the number of filters in each fire module from the beginning to the end of the network.

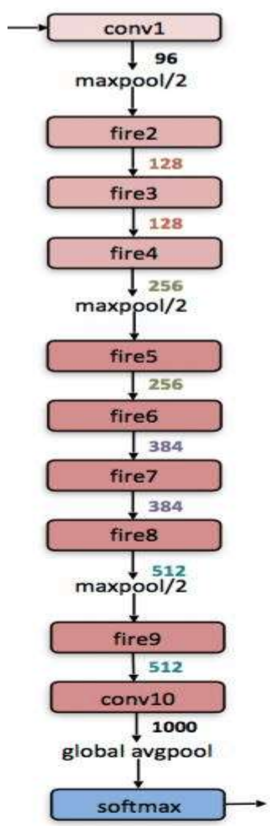


Fig 3 : the architecture of SqueezeNet

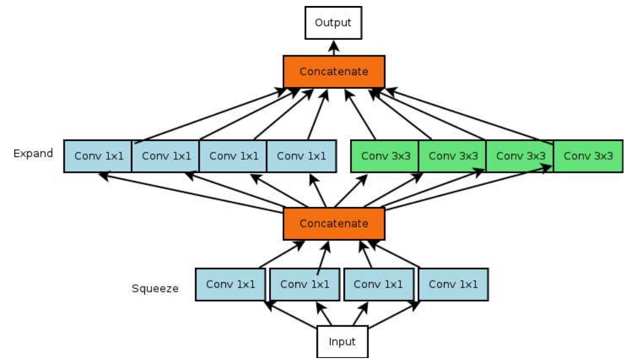


Fig 4 : fire module internal structure

Following model fine-tuning, we used the Dice co-efficient to evaluate the model. The dice score is the result of dividing the total number of pixels in the two images by twice the overlapped area. Dice score is the standard metric for image segmentation.

## IV. Results

The KITS-19 data set is used in this study. The data set's images, which are examples of a three-dimensional CT scan, may or may not include kidneys. The ResNet and SqueezeNet models used achieved dice scores of 99.05 and 97.58 percent, respectively. The ResNet model required more time to train than the SqueezeNet model. The dataset that has been provided includes both images and segmented masks.

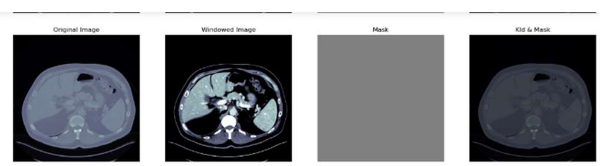

Fig 5 : No kidney identified

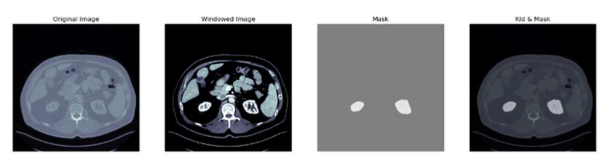

Fig 6 : kidney is identified

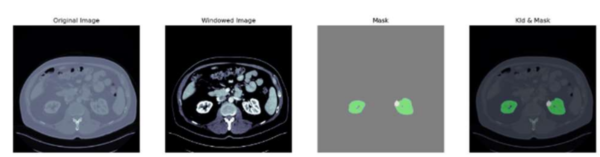

Fig 7 : kidney along with tumor detected

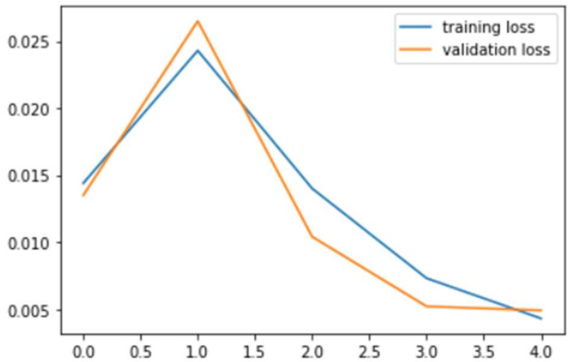


Fig 8 :ResNet model loss graph with epoch on x-axis and loss on y-axis

| epoch | train_loss | valid_loss | dice_multi | time |
|---|---|---|---|---|
| 0 | 0.011236 | 0.005047 | 0.969445 | 06:15 |
| 1 | 0.006502 | 0.002910 | 0.981280 | 06:03 |
| 2 | 0.004554 | 0.002773 | 0.982015 | 06:08 |
| 3 | 0.003690 | 0.002445 | 0.983710 | 06:08 |
| 4 | 0.003247 | 0.002373 | 0.984521 | 06:04 |
| 5 | 0.008610 | 0.051644 | 0.856550 | 06:05 |
| 6 | 0.083472 | 0.032310 | 0.625152 | 06:02 |
| 7 | 0.043335 | 0.004020 | 0.978933 | 06:03 |
| 8 | 0.020856 | 0.002174 | 0.985346 | 06:03 |
| 9 | 0.010576 | 0.001815 | 0.986738 | 06:02 |
| 10 | 0.005812 | 0.001743 | 0.987805 | 06:00 |
| 11 | 0.003709 | 0.001643 | 0.988363 | 06:00 |
| 12 | 0.002674 | 0.001445 | 0.989325 | 05:57 |
| 13 | 0.002105 | 0.001318 | 0.989974 | 05:59 |
| 14 | 0.001878 | 0.001366 | 0.989824 | 06:05 |
| 15 | 0.001668 | 0.001642 | 0.988366 | 06:54 |
| 16 | 0.001479 | 0.001272 | 0.990591 | 06:54 |
| 17 | 0.001402 | 0.001276 | 0.990743 | 06:52 |
| 18 | 0.001334 | 0.001262 | 0.990807 | 07:37 |
| 19 | 0.001299 | 0.001308 | 0.990568 | 07:30 |

Fig 9 : ResNet Models dice with respect to epochs

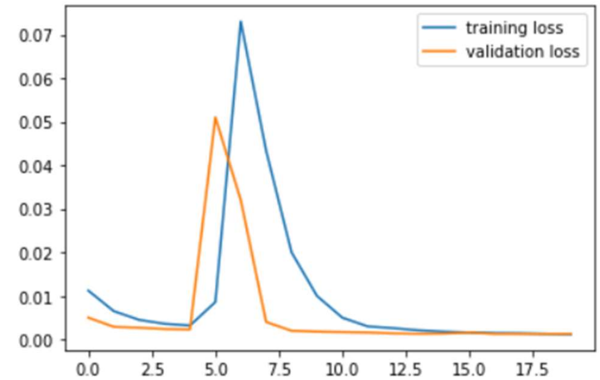


Fig 10 :SqueezeNet model loss graph with epoch on x-axis and loss on y-axis

| epoch | train_loss | valid_loss | dice_multi | time |
|---|---|---|---|---|
| 0 | 0.014465 | 0.013511 | 0.943626 | 44:32 |
| 1 | 0.024302 | 0.036575 | 0.848023 | 1:00:30 |
| 2 | 0.014034 | 0.007459 | 0.963995 | 39:04 |
| 3 | 0.007342 | 0.005232 | 0.972922 | 39:12 |
| 4 | 0.004329 | 0.004913 | 0.975872 | 39:14 |

Fig 11 : SqueezeNet model dice with respect to epochs

## V. Discussion

Based on the results of the experiments, we can compare the results of techniques that have been studied before and are mentioned in the Literature Survey Section. This table provides a summary of the various strategies with the highest dice scores from each alogirithm.

TABLE I. COMPARISON OF BEST DICE SCORE OBTAINED FROM VARIOUS TECHNIQUES

| Ref No | Algorithm | Dice score |
|---|---|---|
| 17 | AlexNet | 0.92 |
| 18 | DensNet | 0.91 |
| 14 | DafNet | 0.85 |
| 15 | UNet++ | 0.92 |
| 12 | UNet | 0.93 |
| **proposed** | **SqueezeNet** | **0.97** |

## VI. Conclusion

SqueezeNet, the proposed model, outperforms all of the other models, including UNet++, DafNet, AleNet, DenseNet, and UNet, according to the results of the experiments. The advantage of squeezeNet over these models is that it takes less time to train. We can make the models more accurate by providing more data and computing power for training. Brain and liver tumor datasets can also be used with this method.

## VII. References


[1] National kidney foundation https://www.kidney.org/atoz/content/-kidney-cancer

[2] American cancer society https://www.cancer.org/cancer/kidney-cancer/about/what-is-kidney-cancer.html

[3] Qin, Dian & Bu, Jiajun & Liu, Zhe & Shen, Xin & Zhou, Sheng & Jingjun, Gu & Wang, Zhijua & Wu, Lei & Dai, Huifen. (2021). Efficient Medical Image Segmentation Based on Knowledge Distillation.

[4] P. Bilic, et al., "The Liver Tumor Segmentation Benchmark (LiTS)," 2019, arXiv:1901.04056. [Online]. Available:https://arxiv.org /abs/ 1901.04056

[5] N. Heller, et al., "The KiTS19 Challenge Data: 300 Kidney Tumor Cases with Clinical Context, CT Semantic Segmentations, and Surgical Outcomes," 2019, arXiv:1904.00445. [Online]. Available: https:/-/arxiv.org/abs/1904.00445

[6] Iandola, F. N., Moskewicz, M. W., Ashraf, K., Han, S., Dally, W. J., & Keutzer, K. (2016). SqueezeNet: AlexNet-level accuracy with 50x fewer parameters and <1MB model size. CoRR, abs/1602.07360. http://arxiv.org/abs/1602.07360.

[7] Grand Challenge https://kits19.grand-challenge.org/

[8] Brainder https://brainder.org/2012/09/23/the-nifti-file-format/

[9] Squeeze net https://medium.com/@smallfishbigsea/notes-of-squeezenet-4137d51feef4

[10] Kaiming He Georgia Gkioxari Piotr Dollar Ross Girshick ´ Facebook AI Research (FAIR)

[11] Robert J Gillies, Paul E Kinahan, and Hedvig Hricak. Radiomics: images are more than pictures, they are data. Radiology, 278(2):563–577, 2016.

[12] Xiao- Xia Yin , 1,2 Le Sun,3 Yuhan Fu,1 Ruiliang Lu,4 and Yanchun Zhang 1

[13] Patrick Ferdinand Christ, Florian Ettlinger, Felix Grun , Mohamed ¨ Ezzeldin A Elshaera, Jana Lipkova, Sebastian Schlecht, Freba Ahmaddy, Sunil Tatavarty, Marc Bickel, Patrick Bilic, et al. Automatic liver and tumor segmentation of ct and mri volumes using cascaded fully convolutional neural networks. arXiv preprint arXiv:1702.05970, 2017.

[14] Liang- Chieh Chen, George Papandreou, Iasonas Kokkinos, Kevin Murphy, Alan L. Yuille

[15] Sanjay Kumar1, Naresh Kumar2, Rishabh3, Inderpreet Kaur4, Vivek Keshari1

[16] Fausto Milletari 1 , Nassir Navab 1 , 2 , Seyed-Ahmad Ahmadi 3 1 Computer Aided Medical Procedures, Technische Universit¨at M¨unchen, Germany 2 Computer Aided Medical Procedures, Johns Hopkins University, Baltimore, USA 3 Department of Neurology, Klinikum Grosshadern, Ludwig-Maximilians-Universit¨at M¨unchen, Germany

[17] G. Litjens, T. Kooi, B. E. Bejnordi, A. A. A. Setio, F. Ciompi, M. Ghafoorian, J. A. van der Laak, B. V. Ginneken, and C. I. Sanchez, ´ "A survey on deep learning in medical image analysis," Medical Image Analysis, vol. 42, pp. 60–88, 2017.

[18] F. Zhao and X. Xie, "An overview of interactive medical image segmentation," Annals of the BMVA, vol. 2013, no. 7, pp. 1–22, 2013.